 DEAL WE57 0047

Measurement of Chapman-Jouguet Pressure for Explosives*

W. E. DEAL
University of California, Los Alamos Scientific Laboratory, Los Alamos, New Mexico
(Received April 25, 1957)

The Chapman-Jouguet pressures of RDX, TNT, 64/36 Composition B, and 77/23 Cyclotol have been measured by determining initial free-surface velocity as a function of thickness for 24ST aluminum plates in contact with the detonating explosive. An optical technique is described for the measurement of the velocities. The pressures determined for RDX, TNT, 64/36 Composition B, and 77/23 Cyclotol are 338, 189, 292, and 313 kilobars, respectively.

INTRODUCTION

IT was first suggested by Goranson[1] in 1945 that explosive pressures could be established by measurement of the free-surface velocity as a function of thickness for metal plates in contact with the explosive. Duff and Houston[2] reported measurements of this type for Composition B made by an electrical contactor method. This paper will present similar measurements made for RDX, TNT, Composition B, and Cyclotol by an optical technique.

BASIC PRINCIPLES

A steady-state plane detonation wave has been described by Zeldovich,[3] von Neumann,[4] and Döring[5] as a shock followed by a reaction zone of decreasing pressure terminating at the Chapman-Jouguet (C-J) plane. The unsteady flow behind this plane of complete reaction has been described by Taylor[6]; such flow is essentially a rarefaction wave centered at the rear of the explosive. The generally accepted picture of the pressure profile of a detonation wave is thus much like that of Fig. 1.

When such a wave impinges upon an inert material in contact with the explosive, the wave transmitted is a shock followed closely by a steep rarefaction which is in turn followed by a more gradual rarefaction. The shock impedance discontinuity at the interface also causes disturbances (shocks or rarefactions depending on the direction of change of impedance) to be reflected back into the explosive. The effect of this reflected wave on the reaction kinetics and any consequent change in the C-J state is assumed to be negligible in the following discussion. As the transmitted wave travels through the inert material, the steep rarefaction overtakes and eliminates that portion of the wave corresponding to the von Neumann pressure spike. Then in further travel through the material, the rarefaction corresponding to the Taylor wave more gradually overtakes and reduces the pressure of the remaining shock front. Shock front pressure in the inert as a function of the thickness of that material thus varies qualitatively as shown in Fig. 2. Each point of this pressure-thickness curve may be considered as related to a point on the pressure profile of the detonation wave. P_m^*, in particular, corresponds to the pressure at the C-J plane in the detonation wave.

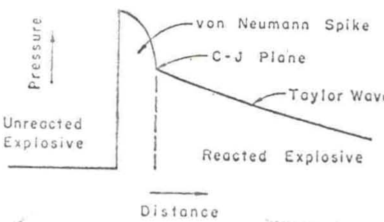

FIG. 1. Generally accepted picture of the pressure profile of a detonation wave.

If one considers the interaction at the explosive-inert material interface as shown in Fig. 3, one can write

$$P_m = P_x + \rho_r{}^0 D_r (U_x - U_m), \tag{1}$$

where P_x is the pressure in the detonation wave, P_m is the induced pressure in the inert material, and the ρ's, U's, and D's are densities, particle velocities, and shock (or detonation) velocities, respectively, particularized by the subscripts: x referring to the detonation wave, m referring to the inert material, and r referring to the reflected wave in the explosive. Conditions in front of these waves are referred to by a superscript zero. All velocities are measured relative to the particle velocities in front of the wave. Then using the momentum conservation equations, $P_x = \rho_x{}^0 U_x D_x$ and $P_m = \rho_m{}^0 U_m D_m$,

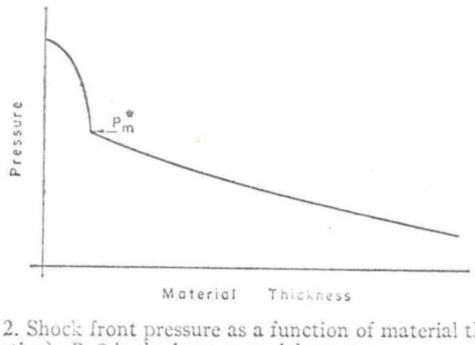

FIG. 2. Shock front pressure as a function of material thickness (qualitative). P_m^* is the inert material pressure corresponding to C-J pressure in the explosive.

* Work done under the auspices of the U. S. Atomic Energy Commission. A version of this paper was presented at the Second Office of Naval Research Symposium on Detonation at Washington, D. C. in February, 1955.

[1] R. W. Goranson, Classified Los Alamos Report LA-487.
[2] R. E. Duff and E. Houston, J. Chem. Phys. 23, 1268 (1955).
[3] Y. B. Zeldovich, J. Exptl. Theoret. Phys. (U.S.S.R.) 10, 542 (1940).
[4] J. von Neumann, OSRD Report No. 549 (1942).
[5] W. Döring, Ann. Physik 43, 421 (1943).
[6] G. I. Taylor, Proc. Roy. Soc. (London) A200, 235 (1950).

one obtains

$$P_m/P_x=[\rho_m{}^0D_m/\rho_x{}^0D_x]\times[(\rho_x{}^0D_x+\rho_r{}^0D_r)/(\rho_m{}^0D_m+\rho_r{}^0D_r)]. \quad (2)$$

If one makes the acoustic approximation $\rho_r{}^0D_r=\rho_x{}^0D_x$, Eq. (2) simplifies to

$$P_x=(P_m/2\rho_m{}^0D_m)(\rho_x{}^0D_x+\rho_m{}^0D_m). \quad (3)$$

Error analysis shows P_x to be quite insensitive to error in $\rho_r{}^0D_r$; for example, in Composition B a 10% error in $\rho_r{}^0D_r$ corresponds only to a 1% error in P_x. A more precise treatment of the interface interaction by W. Fickett and R. D. Cowan[7] gives for the cases of interest in this paper values of explosive pressure only about 1% higher than those resulting from the acoustic approximation.

If in Eq. (3) one identifies P_m as $P_m{}^*$ and P_x as the C-J pressure (P_{cj}) of the explosive, then P_{cj} can be established since $\rho_x{}^0$ and $\rho_m{}^0$ are the simply measurable initial densities of the explosive and the inert, D_x is the

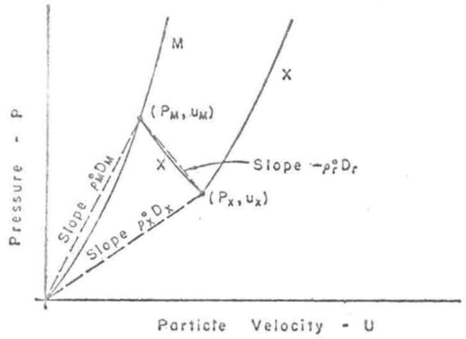

FIG. 3. Interaction at the interface between explosive and inert material in contact with it. M is the inert material Hugoniot; the X's are Hugoniots for the reacted products of the explosive.

readily measurable detonation velocity[8] and $D_m{}^*$ and $P_m{}^*$ are available from equation of state data if one hydrodynamic variable of this state is measured.[9] The quantity established in these experiments was the free-surface velocity ($U_{fs}{}^*$).

An alternative method of establishing the C-J state, which minimizes the hitherto neglected effect of the reflected wave in the explosive on the reaction kinetics, is to establish the $P_m{}^*$ state for each of several inert materials of different shock impedance. The state points define a curve in the pressure-particle velocity plane which closely approximates the locus of all possible shocked and rarefied states (for one direction of wave travel) from the C-J state of the explosive. It differs from this locus only insofar as the wave reflected back into the explosive affects the reaction kinetics; however, the amplitude of the reflected wave approaches zero as

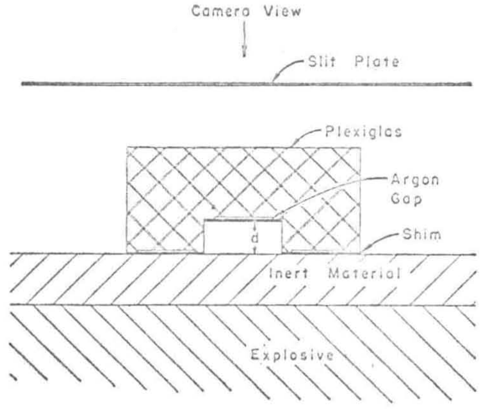

FIG. 4. Plexiglas block assembly for measurement of free-surface velocity of an explosive-driven plate.

one approaches the C-J state on this curve. The C-J state must also lie on the line $P_{cj}/U_{cj}=\rho_x{}^0D_x$ (where U_{cj} is the C-J particle velocity). The C-J point is thus established as the intersection of this line with the aforementioned curve at the point where the perturbation of the reaction by a reflected wave is minimized.

EXPERIMENTAL TECHNIQUE

The value of free-surface velocity corresponding to $P_m{}^*$ for a given explosive and inert material was determined by measurement of free-surface velocity of an explosive-driven plate as a function of plate thickness. These velocities were measured photographically by use of a rotating-mirror smear camera with a writing speed of 3.2 mm/μsec. A Plexiglas block assembly such as that of Figs. 4 and 5 was placed on the surface to be studied. This was viewed by the camera through a slit and swept on the film in a direction perpendicular to the slit image. When the explosive-driven plate on which such an assembly is placed begins to move, the argon gaps near the plate surface are closed first and yield a brilliant

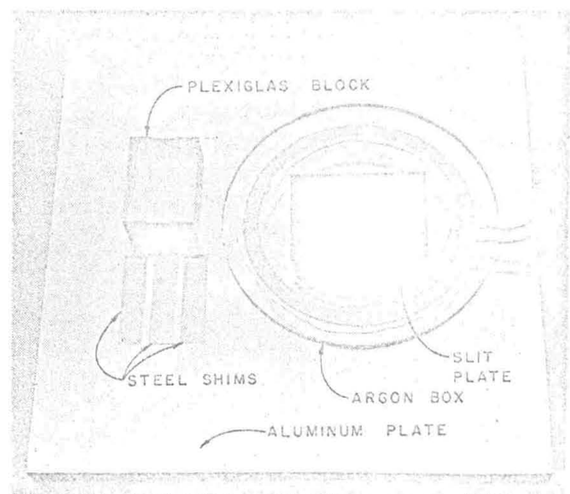

FIG. 5. Disassembled parts of the plate assembly for a free-surface velocity record such as shown in Fig. 6.

[7] R. D. Cowan and W. Fickett, J. Chem. Phys. 24, 932 (1956).
[8] Campbell, Malin, Boyd, and Hull, Rev. Sci. Instr. 27, 567 (1956).
[9] Walsh, Rice, McQueen, and Yarger, Phys. Rev. (to be published).

FIG. 6. Smear camera record showing seven records of free-run time of a metal plate accelerated by explosive. Free-run time is measured from each pair of the side traces down to the corresponding central plate arrival time.

flash of light of short duration. After the free surface moves the distance d, it closes the central gap and yields another flash of light. The time between these light flashes is the free-run time. The gaps and shims were made as nearly identical as possible so as to maintain identical gap closure time for the side reference traces and the central data trace. All gaps on a single block were machined with one shaped cutter and were usually 0.0035 in. deep. A variety of shim materials were tried and performed satisfactorily, but the flatness and convenient availability of steel feeler gauge stock (in 0.003 to 0.005 in. thicknesses) made it the most used. Good contact of the shim to both the plate and block was assured by holding flatness tolerances over the contact

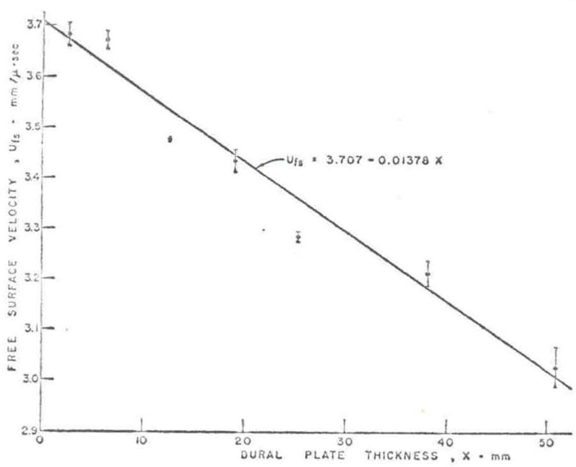

FIG. 7. Experimental values of free-surface velocity imparted to 24ST aluminum plates by pressed, high-density RDX as a function of plate thickness. The line shown is the linear least squares fit to the data.

surfaces to ±0.0002 in. The widths of the central offset in the blocks were chosen such that no disturbance arising at either of the adjacent Plexiglas corners in contact with the plate could perturb either the motion

TABLE I. Experimental free-surface velocities of various thicknesses of 24ST aluminum for four explosives. Errors quoted are standard deviations of the mean.

24ST aluminum thickness, X (mm)	Free-surface velocity U_{fs} (mm/μsec)	Number of data points
	RDX	
2.51	3.682±0.022	7
6.31	3.671±0.018	7
12.69	3.476±0.005	5
19.09	3.434±0.022	5
25.37	3.284±0.010	5
38.13	3.212±0.025	5
50.80	3.027±0.039	5
	TNT	
2.53	2.470±0.006	7
6.43	2.422±0.009	7
12.73	2.371±0.008	7
19.05	2.363±0.011	7
24.87	2.288±0.006	6
38.10	2.193±0.003	4
50.88	2.157±0.007	8
	64/36 Composition B	
1.85	3.414±0.019	3
2.54	3.389±0.014	5
3.16	3.378±0.013	3
3.77	3.343±0.011	4
5.02	3.335±0.006	9
6.34	3.316±0.010	14
7.61	3.290±0.012	5
8.48	3.281±0.022	4
10.02	3.284±0.005	32
11.31	3.256±0.019	4
12.23	3.240±0.010	4
12.68	3.241±0.005	32
19.14	3.182±0.008	15
23.98	3.156±0.014	8
25.58	3.085±0.007	5
38.33	2.961±0.010	5
50.88	2.860±0.015	10
	77/23 Cyclotol	
1.90	3.545±0.008	3
2.53	3.528±0.013	4
3.13	3.534±0.026	5
3.80	3.494±0.013	4
4.92	3.477±0.013	5
6.32	3.447±0.010	6
7.74	3.451±0.010	5
8.88	3.431±0.024	4
9.92	3.420±0.011	5
11.26	3.426±0.003	6
12.43	3.369±0.015	4
19.05	3.287±0.011	5
24.41	3.280±0.010	6
38.17	3.142±0.003	5
50.85	3.027±0.012	5

of the central region of the plate section moving across the free-run gap or the gap closure mechanism. The depth of the offset was chosen so that all measurements were taken before shock reverberations could occur. This requirement, in particular, makes precision meas-

urement on p
technique. Th
and was also
Plexiglas we
velocity.
The Plexig
shims while
Extreme car
and prevent
surfaces. In m
of free-surfac
many as twel
assembly of t
containing b
slit plate was
In all exp
plosive to be
of eight inch
type of lens

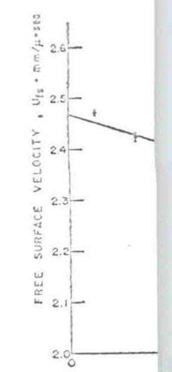

FIG. 8. Expe
24ST aluminur
of plate thickn
the data.

explosive to
of initial den
All explosive
±0.0005 in.
sulting from
film of mine
sembly with
Such recor
at 100 or m
polation bet
time of depa
with the cen
velocity thr
offset. Such
plate thickn
studied. No
the entire ra
study is of a

ne central offset
no disturbance
glas corners in
ther the motion

s of various thick-
Errors quoted are

Number of data points
7
7
5
5
5
5
5
7
7
7
7
6
4
8
3
5
3
4
9
14
5
4
32
4
4
32
15
8
5
5
10
3
4
5
4
5
6
5
4
5
6
4
5
6
5
5

n moving across
mechanism. The
ll measurements
ns could occur.
precision meas-

urement on plates thinner than 1 mm difficult by this technique. The shock reverberation time was calculated and was also checked in preliminary experiments using Plexiglas wedges so as to continuously record plate velocity.

The Plexiglas blocks were glued to the plates and shims while clamped together under slight pressure. Extreme care was taken to eliminate all dust particles and prevent glue from getting between the contacting surfaces. In most individual shots several measurements of free-surface velocity were taken; in some shots as many as twelve thicknesses were studied at once. After assembly of the blocks on a plate, a transparent argon-containing box was cemented over the assembly; the slit plate was taped in place on this box.

In all experiments reported here the blocks of explosive to be studied were initiated by plane wave lenses of eight inch aperture. The major component of this type of lens and that component in contact with the

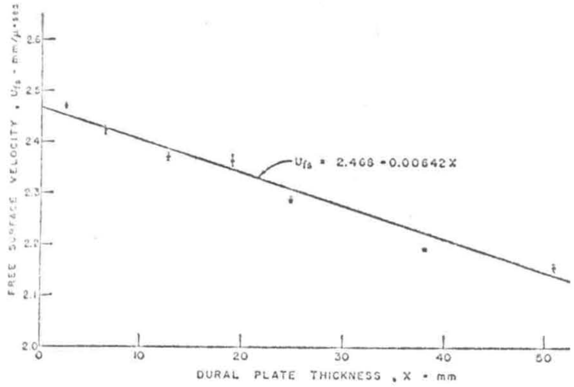

FIG. 8. Experimental values of free-surface velocity imparted to 24ST aluminum plates by pressed high-density TNT as a function of plate thickness. The line shown is the linear least squares fit to the data.

explosive to be studied was barium nitrate loaded TNT of initial density 2.6 g/cc and C-J pressure 140 kilobars. All explosive contacting surfaces were flat planes within ±0.0005 in. Any air gaps at explosive interfaces resulting from these tolerances were eliminated by a thin film of mineral oil. A print of a film record for an assembly with seven slits is shown as Fig. 6.

Such records were read on a comparator and plotted at 100 or more times film time scale; graphical interpolation between the two side reference traces yielded a time of departure of the central free-surface which along with the central trace gave a transit time and hence velocity through the precisely measured depth of the offset. Such velocity data were taken for a variety of plate thicknesses out to 50 mm for each of the explosives studied. No particular effort was made to take data over the entire range of thicknesses on a single shot, since the study is of a type of explosive, not a single piece.

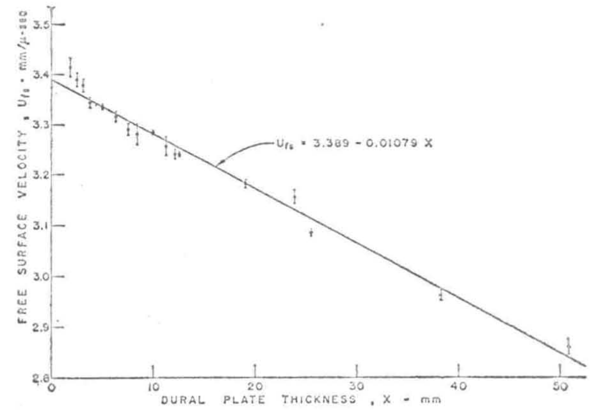

FIG. 9. Experimental values of free-surface velocity imparted to 24ST aluminum plates by 64/36 Composition B as a function of plate thickness. The line shown is the linear least squares fit to the data.

EXPERIMENTAL DATA AND RESULTS

Charges of RDX, TNT, 64/36 Composition B, and 77/23 Cyclotol were studied. The RDX (cyclotrimethylene trinitramine) charges were six inches thick made up of two cylinders six inches in diameter and three inches thick pressed without a binder to 98% of crystal density from a granular RDX of 100 μ median particle size. The TNT (trinitrotoluene) charges were truncated cones eight inches thick of eight inch diameter at the small end and thirteen inch diameter at the large end; these were initiated from the small end. They were pressed without binder to 99% of crystal density from a granular TNT of about 400 μ median particle size. The Composition B and Cyclotol charges were eight inches thick; individual shot charges were made up of two 10×10×4 in. blocks, each of which was machined from a casting. The Composition B was 64.1±0.6% RDX; the Cyclotol was 77.0±1.0% RDX. These compositions were based on samples taken from castings identical to those fired. The other constituent in the latter two explosives was TNT.

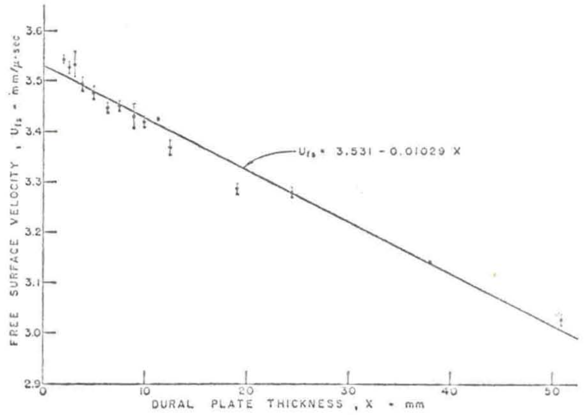

FIG. 10. Experimental values of free-surface velocity imparted to 24ST aluminum plates by 77/23 Cyclotol as a function of plate thickness. The line shown is the linear least squares fit to the data.

TABLE II. Explosive data and calculated results. Errors quoted are standard deviations.

Explosive	RDX	TNT	64/36 Composition B	77/23 Cyclotol
Explosive density, ρ_x^0, (g/cc)	1.767 ± 0.011	1.637 ± 0.003	1.713 ± 0.002	1.743 ± 0.001
Detonation velocity, D_x, (mm/μsec)	8.639 ± 0.041	6.942 ± 0.016	8.018 ± 0.017	8.252 ± 0.017
24ST aluminum density, ρ_m^0, (g/cc)	2.788 ± 0.008	2.790 ± 0.003	2.791 ± 0.004	2.793 ± 0.006
24ST aluminum free-surface velocity, U_{fs}^*, (mm/μsec)	3.693 ± 0.016	2.462 ± 0.006	3.378 ± 0.004	3.521 ± 0.005
24ST aluminum shock velocity, D_m^*, (mm/μsec)	7.809 ± 0.023	7.001 ± 0.018	7.604 ± 0.019	7.697 ± 0.019
24ST aluminum pressure, P_m^*, (kilobars)	$397.3\ \pm2.4$	$239.1\ \pm0.9$	$354.8\ \pm1.8$	$374.4\ \pm2.0$
C-J pressure, P_{cj}, (kilobars)	$337.9\ \pm3.1$	$189.1\ \pm1.0$	$292.2\ \pm2.6$	$312.5\ \pm2.9$
C-J particle velocity, U_{cj}, (mm/μsec)	2.213 ± 0.029	1.664 ± 0.011	2.127 ± 0.019	2.173 ± 0.020

The free-surface velocities measured for various thicknesses of 24ST aluminum for the explosives studied are listed in Table I and plotted on Figs. 7 through 10. The error flags shown on these figures are standard deviations of the averages and do not include consistent error estimates. All of the individual data points for each explosive were used in a linear least squares fit to the data. The resulting fits are given on the figures. The use of straight lines fits is only justified by how well the data do fit these lines. The metal thickness corresponding to the explosive reaction zone is not established in these experiments; hence a plate thickness of 1.0 mm is chosen in accordance with the results of Duff and Houston[2] for Composition B. The metal state corresponding to the explosive C-J state is thus given as the 1.0-mm point on the least squares line. These aluminum free-surface velocities (U_{fs}^*) are given in Table II along with measured values of ρ_m^0, ρ_x^0, and D_x; values D_m^* and P_m^* deduced from the measured Hugoniot[8]; and values of P_{cj} and U_{cj} calculated from the other numbers given.

The errors quoted in Table II for ρ_m^0, ρ_x^0, and D_x are the standard deviations of these quantities among the plates and charges used. The error quoted for U_{fs}^* is the standard deviation of the least squares fit; this should include the contribution from an estimated $\pm\frac{1}{2}\%$ error in the individual measurements. The standard deviations quoted for other quantities are deduced from these errors with an additional $\frac{1}{4}\%$ contribution to the D_m error as an estimate of the precision of the Hugoniot data.

If one corrects the Duff and Houston[2] value of P_{cj} (272 Kb) for Composition B of 63% RDX and 1.67 g/cc to the 64.1% RDX and 1.713 g/cc of this paper using the semiempirical corrections; $\delta P_{cj}/P_{cj}=2.30\delta\rho_x^0/\rho_x^0$ and $\delta P_{cj}=1.57$ Kb per % RDX; one obtains a P_{cj} of 290 Kb, a value in excellent agreement with the one reported here.

ACKNOWLEDGMENTS

This work was made possible only through the cooperation of many members of GMX Division of the Los Alamos Scientific Laboratory.